

Raman overtone intensities measured for H₂

D. P. Shelton

Department of Physics, University of Nevada, Las Vegas, Las Vegas, Nevada 89154

(Received 26 February 1990, accepted 16 April 1990)

The Raman spectra of the vibrational fundamental, first overtone and second overtone transitions of the H₂ molecule were recorded using visible and ultraviolet argon-ion laser excitation. The ratios of transition polarizability matrix elements, $\alpha_{01,21}/\alpha_{01,11}$ and $\alpha_{01,31}/\alpha_{01,11}$, were determined from the measured intensities of the $Q(1)$ Raman lines $\nu, J = 0, 1 \rightarrow \nu', 1$ for $\nu' = 1, 2, 3$. The experimentally determined value of the Raman first overtone matrix element is in good agreement with the value from the best *ab initio* calculation.

INTRODUCTION

Overtone transitions are rarely observed in Raman spectroscopy. The overtone transitions are usually too weak to observe unless they are enhanced by a resonance with a neighboring fundamental transition (e.g., $2\nu_6$ and ν_1 for SF₆),¹ or due to coincidence of the incident light frequency with a vibronic transition frequency (e.g., resonance Raman spectrum of I₂).² The only published observations of unenhanced Raman vibrational transitions for diatomic molecules are the result of recent experiments with D₂, N₂, and O₂.³

In the experiments reported by Knippers *et al.*³ the intensity of the first vibrational overtone transition for D₂ was measured and found to be less than half the value predicted by *ab initio* calculation. This large discrepancy is disturbing since an accurate comparison of theory and experiment is straightforward and apparently unequivocal in this case, and because hydrogen and its isotopes play a special role in molecular physics because their properties can be calculated quite accurately from first principles.^{4,5} For example, the *ab initio* transition polarizability matrix element for the $S(1)$ rotational Raman line of H₂ is presently the primary standard for all gas phase Raman cross section determinations.⁶ In attempting to understand the origin and assess the possible implications of the discrepancy observed for the overtone intensity of D₂, comparison with the corresponding result for H₂ would be most instructive. However, the overtone transition for H₂ was unobservable in the previous experiments because the overtone Raman line was red-shifted out of the sensitive spectral range of the detector. Therefore we have undertaken to measure the Raman overtone intensities for H₂ in order to confirm and refine the observations of the previous workers and to assess possible inadequacies of the existing calculations.

EXPERIMENTAL METHOD

The experiments employ the usual apparatus for spontaneous Raman scattering measurements at 90° scattering angle. The light source is an argon-ion laser whose beam is focused to produce a beam waist with a diameter of 100 μ m, centered in the sample cell, and making a single pass through the sample cell. The light scattered from the focal region into a cone of 9° half-angle is collected by a lens, and imaged with 2.5 times linear magnification onto the entrance slit of a Jo-

bin-Yvon Ramanor U 1000 double monochromator with f/8 optics (the long axis of the slit is horizontal and parallel to the laser beam). A compensator and prism polarizer are used to adjust the laser beam polarization vector (**E**) so that it is vertical as the beam passes through the sample. A sheet polarizer placed before the monochromator entrance slit selects only vertically polarized scattered light (VV polarization geometry). The detector is a photomultiplier tube having high sensitivity over the range 200 < λ < 900 nm (cooled Hamamatsu R943-02, with GaAs:Cs photocathode), operated in photon counting mode. To accumulate a Raman spectrum, the photomultiplier output pulses are fed to a multichannel scaler whose channel advance is synchronized with the scan of the monochromator gratings.

For most measurements, the sample cell was filled with H₂ gas (99.999% purity) at 10 atm pressure and at room temperature (26–28 °C). The density dependence of the integrated intensity of the first overtone $Q(1)$ line was measured for sample pressures in the range 1–11 atm, and no significant deviation from $I/\rho = \text{constant}$ was detected at the 2% level of accuracy. The observed linearity of the scattered intensity vs density up to at least 10 atm means that systematic errors due to intermolecular interactions are not introduced by using high sample density to increase the strength of the Raman signal. Measurements were made with laser excitation wavelengths of 488.0, 457.9, 363.8, and 351.1 nm, and Raman lines were observed at wavelengths over the range 805 > λ > 410 nm. The laser beam power entering the sample cell was 1.5 W when operating in the visible and 0.4 W when operating in the ultraviolet, generating peak Raman count rates of about 6000, 600, and 6 cps for the fundamental, first, and second overtones, respectively (above the 6 cps photomultiplier tube background count rate). The range of signal intensities was compressed by inserting optical filters with up to 10 times attenuation in front of the entrance slit of the spectrometer (filter transmission was calibrated *in situ*). Corrections for the dead time of the photon counting electronics were determined and applied (maximum correction about 2%). The spectrometer slit widths were set at 250 μ m for the first monochromator and 500 μ m for the second monochromator (slit lengths were 20 mm). Choosing wide but unequal slit widths allows 95% of the light collected from the sample to enter the spectrometer and makes the transmission of the tandem monochromators

quite insensitive to tracking errors. The spectral slit width is wavelength dependent, varying from 1.2 cm⁻¹ at the red end of our range to 6.3 cm⁻¹ at the blue end. The integrated intensity of a Raman line is determined by scanning over the line (typical scan duration 200 s) and computing the total counts above background for the recorded peak. When comparing two Raman lines, they are scanned in alternation so that the effects of drifts in experimental parameters such as laser alignment will tend to cancel.

To extract the Raman scattering cross section from the measured integrated intensity one must know the spectral response function of the measuring instrument. The spectral response of our spectrometer is determined by means of a calibrated incandescent tungsten ribbon lamp (General Electric 20A/T-24/2 operated at 13 A), as outlined in Ref. 7 (with several misprints). The calibration data for this lamp fits the spectral radiance for a tungsten surface at $T = 2413$ K (calculated using tabulated emissivities from Ref. 8) with a standard deviation of 2.5% in the relative intensity over the range $400 < \lambda < 1000$ nm. The uncertainty of the filament temperature obtained from this fit is conservatively estimated as ± 30 °C. The spectral response of the Raman spectrometer is determined assuming the lamp radiance is given by the smooth calculated spectral radiance function for a tungsten gray body at the best fit temperature; the assessed uncertainty in the ratio of lamp spectral radiance at two wavelengths is based on the estimated filament temperature uncertainty.

The apparatus is arranged so that one may optically substitute the calibration light source for the Raman scattering source without adjusting any optical elements. Light from the calibrated lamp is diffusely reflected from a white reflector (Kodak 6080 white reflectance coating) of known high spectral reflectance. The surface of this reflecting screen is imaged with unit magnification by a pair of uncoated lenses. The image is formed at the position of the laser beam waist inside the sample cell, with the light entering through an uncoated fused silica window placed directly opposite the sample cell window through which the Raman light exits. The transmission through the optical elements between the lamp and the Raman source position is accurately calculable, so the spectrum of the lamp light at the Raman source position is known. The white reflecting screen allows one to attenuate the otherwise excessively bright lamp light in a spectrally neutral fashion by simply adjusting the distance between the lamp and screen, while the lenses are needed to ensure that the calibration light overfills the spectrometer entrance aperture to the same extent as the Raman light. Precautions are taken to ensure that only light from the lamp, following the specified optical path, contributes to the calibration signal.

The Raman light is highly polarized and nearly monochromatic whereas the light from the lamp is unpolarized and broadband. Because of the strong polarization selectivity of the spectrometer and the imperfect selectivity of the polarizer, it is necessary to measure the wavelength-dependent polarization response of both elements in order to deduce the polarized-light spectral response of the polarizer and spectrometer combination from measurements employing

the unpolarized light source. The required information is obtained at the wavelength of each of the observed Raman lines from four measurements: signal with and without a second polarizer following the first polarizer, for both V and H orientations of the first polarizer pass axis. The maximum resulting spectrometer response correction is 9%. The broadband nature of the calibration light source is actually an asset in the determination of the monochromatic-line spectral response function of the spectrometer. For a flat spectral distribution, the measured count rate is proportional to the product of spectral intensity per unit frequency and spectral slit width $\Delta\nu$, while for a monochromatic source, the integrated count obtained by scanning the spectral line at a constant rate $d\nu/dt$ is also proportional to the product of line intensity and spectral slit width. Thus, the wavelength-dependent spectral slit width cancels out in the ratio and does not explicitly enter the calibration. Note that in order to correctly calibrate the spectrometer response per photon, the blackbody distribution function in the expression for the lamp spectrum must be rewritten in the form which gives the photon flux per unit frequency interval.

In these experiments we were able to measure ratios of Raman intensities, corrected for instrumental spectral response variations, with an overall accuracy of about $\pm 5\%$. The contribution to the overall error bar due to the lamp calibration uncertainty is typically 3 times larger than the combined uncertainty due to all other sources (such as the uncertainties in filter transmission, spectrometer polarization response, Raman signal ratio, and lamp signal ratio). The integrated intensity measurements are relatively uncomplicated and reliable since we are measuring sharp, cleanly separated spectral peaks with no significant overlapping spectral features.

RESULTS AND DISCUSSION

Our study focuses on the $Q(1)$ lines of the fundamental and overtone bands since $\frac{2}{3}$ of the total intensity of each band resides in this single line. The $Q(1)$ transitions ($\nu = 0, J = 1$) \rightarrow ($\nu = \Delta\nu, J = 1$) for $\Delta\nu = 1, 2$, and 3 occur with Raman shifts of 4156, 8077, and 11767 cm⁻¹. The Raman shift for $Q(1)\Delta\nu = 3$ is so large that ultraviolet (UV) excitation must be used to bring the Stokes line within the sensitive spectral range of our spectrometer. With UV excitation, the poor spectral resolution of the spectrometer in the blue makes it more difficult to ensure that $Q(1)\Delta\nu = 1$ is observed as an isolated peak, so in this case an extra measurement step with narrower slits and using $Q(3)\Delta\nu = 1$ as a transfer standard is included in the determination of the $Q(1)\Delta\nu = 2$ vs $Q(1)\Delta\nu = 1$ intensity ratio. The determination of the $Q(1)\Delta\nu = 3$ vs $Q(1)\Delta\nu = 2$ ratio is straightforward, but requires 10 times longer scan time for the weak $Q(1)\Delta\nu = 3$ line. Each peak was measured at least three times. The results of these intensity measurements are summarized in Table I.

In addition to the measurements of the relative intensities of the $Q(1)$ lines for transitions to successively higher vibrational states, several other measurements were made as checks on our procedures. Relative intensities and frequency

TABLE I. Measured Raman intensities I and transition polarizability matrix elements α for the $Q(1)$ vibrational transitions of H₂ are given below. The results are expressed as ratios with I and α for the fundamental ($\Delta v = 1$) transition. The intensity I is a measure of the Raman scattering cross section (scattered-photon/incident-photon/molecule). The scattering cross section, for the experimentally selected polarization geometry and initial molecular state, is determined by the combination $\alpha^2 = \bar{\alpha}^2 + (8/225)\Delta\alpha^2$, where $\bar{\alpha}$ and $\Delta\alpha$ are the mean polarizability and its anisotropy for the particular transition. Wavelengths λ are those measured in air, while wave numbers ν are those measured in vacuum.

λ_p (nm)	ν_p (cm ⁻¹)	$\frac{I_{Q(1)\Delta v}}{I_{Q(1)\Delta v=1}}$		$\left \frac{\alpha_{01,\nu'1}}{\alpha_{01,11}} \right $	
		$\Delta v = 2$	$\Delta v = 3$	$\nu' = 2$	$\nu' = 3$
488.0	20 487	$3.26 \times 10^{-3} (\pm 4\%)$...	$0.0862 (\pm 2\%)$...
457.9	21 831	$3.65 \times 10^{-3} (\pm 4\%)$...	$0.0880 (\pm 2\%)$...
363.8	27 481	$4.39 \times 10^{-3} (\pm 3\%)$	$4.08 \times 10^{-5} (\pm 6\%)$	$0.0873 (\pm 1.5\%)$	$0.011 53 (\pm 3\%)$
351.1	28 473	$4.59 \times 10^{-3} (\pm 3\%)$	$4.41 \times 10^{-5} (\pm 6\%)$	$0.0882 (\pm 1.5\%)$	$0.011 66 (\pm 3\%)$

shifts were measured for the $Q(0)$, $Q(1)$, $Q(2)$, and $Q(3)$ lines for $\Delta v = 1$ and $\Delta v = 2$, using $\lambda = 488.0$ nm excitation. The line spacings within a band were found to agree with the predicted positions^{9,10} to about 0.1 cm⁻¹, while the relative intensities were found to agree with the calculated intensities⁹⁻¹¹ to within 5% (the intensity variation within a Q branch is dominated by the rotational population distribution factor). The intensity ratio for the $Q(3)$ and $Q(1)$ lines of the fundamental band was measured more carefully using $\lambda = 363.8$ nm excitation and was found to agree with the calculated ratio to about 1.5%. The residual discrepancy could be accounted for by a 1.5 °C difference between actual sample temperature and the reading of the externally mounted thermometer.

The Raman intensities (in photons/s) that we have measured are related to the transition polarizability matrix elements according to the relation^{4,11,12}

$$I_{\nu J, \nu' J'} \propto \rho(\nu, J) \nu \nu_s^3 \alpha_{\nu J, \nu' J'}^2, \quad (1)$$

where $\rho(\nu, J)$ is the fractional population of the initial rovibrational level, ν and ν_s are the incident and scattered light frequencies, and for $\Delta J = 0$ transitions, α^2 is shorthand for

$$\alpha^2 = \bar{\alpha}^2 + \frac{4}{45} \frac{J(J+1)}{(2J-1)(2J+3)} \Delta\alpha^2. \quad (2)$$

The factor $4/45$ results for the choice of VV polarization geometry, and $\bar{\alpha} = (\alpha_{\parallel} + 2\alpha_{\perp})/3$ and $\Delta\alpha = (\alpha_{\parallel} - \alpha_{\perp})$ are the mean polarizability and the anisotropy for a linear molecule. Since we are comparing transitions originating from the same initial state, the ratios of matrix elements for the $Q(1)$ lines are given in terms of the measured intensities by

$$|\alpha_{01,\nu'1}/\alpha_{01,11}| = (\nu_s^{-3} I_{01,\nu'1})^{1/2} / (\nu_s^{-3} I_{01,11})^{1/2}. \quad (3)$$

The polarizability ratios deduced from our measurements are given in Table I.

In order to compare the experimentally measured polarizability ratios with the results of the *ab initio* calculations, one must account for the frequency dependence of $\alpha_{\nu J, \nu' J'}$. The usual quantum mechanical expression¹² for the $\alpha\beta$ Cartesian tensor component of the Raman tensor may be rearranged into a more symmetrical form:

$$\begin{aligned} \alpha_{mn}^{\alpha\beta}(\omega_s; \omega_p) &= \hbar^{-1} \sum_e \mu_{me}^{\alpha} \mu_{en}^{\beta} \left(\frac{1}{\Omega_{me} - \omega_p} + \frac{1}{\Omega_{me} + \omega_s} \right) \\ &= \hbar^{-1} \sum_e \frac{\mu_{me}^{\alpha} \mu_{en}^{\beta}}{\Omega_{me} + \Omega_{ne}} \\ &\quad \times \left(\frac{1}{1 - (\omega_p + \omega_s)^2 / (\Omega_{me} + \Omega_{ne})^2} \right), \quad (4) \end{aligned}$$

where m and n label the initial and final rovibrational states, e labels the excited electronic states, μ_{me}^{α} is a transition dipole matrix element, Ω_{me} is a molecular transition frequency, and ω_p and ω_s are the incident and scattered light frequencies. The symmetrical form of Eq. (4) allows one to derive the simple dispersion formula:

$$\alpha_{\nu J, \nu' J'}(\nu_s; \nu_p) = \alpha_{\nu J, \nu' J'}(0; 0) [1 + A(\nu_p + \nu_s)^2 + \dots]. \quad (5)$$

The *ab initio* calculations^{9,10} in which overtone matrix elements for H₂ were obtained did not employ the sum-over-states expression of Eq. (4), but instead calculated the transition polarizability matrix elements by vibrational averaging of the clamped-nucleus polarizability function $\alpha(\omega; R)$. The relation between ω appearing in the vibrational-averaged polarizability $\alpha_{\nu J, \nu' J'} = \langle \nu J | \alpha(\omega; R) | \nu' J' \rangle$ and ω_p and ω_s in the Raman scattering event is $\omega = (\omega_p + \omega_s)/2$.

To get an indication of the frequency dependence of the experimental polarizability ratios it is sufficient to plot the data as a function of the average frequency squared,

$$\nu_{av}^2 = [(\nu_p + \nu_s')^2 + (\nu_p + \nu_s'')^2]/8, \quad (6)$$

where s' and s'' denote the Raman-shifted light for the fundamental and overtone transitions, respectively. One is forced to pick such an arbitrary form for the independent variable of the plot because the Raman measurements from which the ratios are determined are made at fixed ω_p , not at constant $(\omega_p + \omega_s)^2$. The polarizability ratio data is plotted vs ν_{av}^2 in Fig. 1, where one sees that the polarizability ratios are in fact only weakly frequency dependent. The weak frequency dependence makes the lack of rigorous justification for ν_{av}^2 less important.

Static transition polarizabilities and polarizability ratios

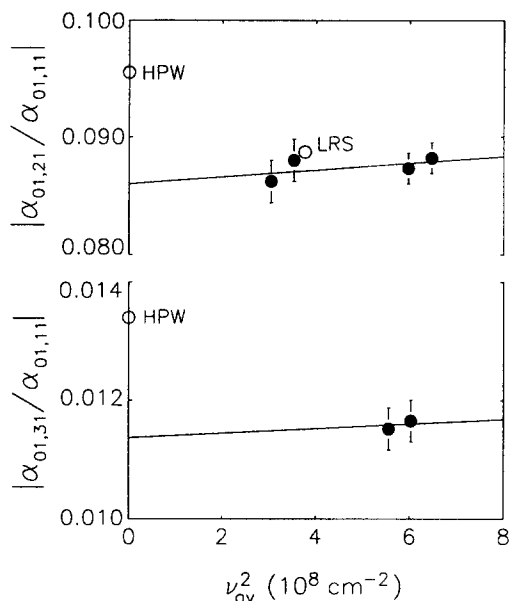


FIG. 1. Measured ratios of Raman overtone and fundamental vibrational transition matrix elements for H₂ (filled circles) are plotted vs the average frequency squared ν_{av}^2 (see text). Extrapolation to the static limit gives $|\alpha_{01,21}/\alpha_{01,11}| = 8.60 \times 10^{-2}$ and $|\alpha_{01,31}/\alpha_{01,11}| = 1.14 \times 10^{-2}$. The results of the static (HPW, Ref. 9) and dynamic (LRS, Ref. 10) *ab initio* calculations are also shown for comparison (open circles).

from the calculation of Hunt, Poll, and Wolniewicz⁹ are given in Table II. The ratios are also plotted in Fig. 1. A straight line fit to the experimental points for $|\alpha_{01,21}/\alpha_{01,11}|$ allows one to extrapolate the experimental results to the static limit for comparison with the *ab initio* results. The experimental estimate, $|\alpha_{01,21}/\alpha_{01,11}| = 8.60 \times 10^{-2} (\pm 3\%)$, is 11% below the *ab initio* result. Extrapolation to the static limit of $|\alpha_{01,31}/\alpha_{01,11}|$ is done by means of a straight line passing through the data points; the relative slope of the line is chosen to be the same as that of the line fitted to the $|\alpha_{01,21}/\alpha_{01,11}|$ data. This extrapolation gives an experimental estimate which is 18% below the static *ab initio* result for $|\alpha_{01,31}/\alpha_{01,11}|$. These discrepancies are too large to be accounted for by possible systematic errors in the extrapolation procedures.

Dynamic transition polarizabilities at $\lambda = 488.0$ nm, from the calculation of LeRoy and Schwartz,¹⁰ are given in Table II. In order to compute polarizability ratios which are

TABLE II. *Ab initio* values of matrix elements and ratios for $Q(1)$ Raman transitions, where $\alpha^2 = \bar{\alpha}^2 + (8/225)\Delta\alpha^2$. The wavelength λ corresponds to the frequency $\omega = (\omega_p + \omega_s)/2$ at which the matrix elements were calculated. A small dispersion adjustment has been applied to the ratio $|\alpha_{01,21}/\alpha_{01,11}|$ at optical frequencies to make it correspond to the polarizability ratio measured with fixed incident light frequency ($\lambda_p = 407.7$ nm, see text).

λ (nm)	$ \alpha_{01,11} $ (au)	$ \alpha_{01,21} $ (au)	$ \alpha_{01,31} $ (au)	$\frac{ \alpha_{01,21} }{ \alpha_{01,11} }$	$\frac{ \alpha_{01,31} }{ \alpha_{01,11} }$
∞^a	0.7492	0.0715	0.0100	0.0955	0.0134
488.0 ^b	0.7994	0.0714	...	0.0887	...

^a Reference 9.

^b Reference 10.

directly comparable with the experimental results, it is necessary to make a small dispersion correction. However, the relevant off-diagonal matrix elements were only calculated at a single frequency. Using the available data, one may estimate that the ratio of dynamic ($\lambda = 488.0$ nm) and static values of $\alpha_{01,11}$ is approximately equal to the average of the corresponding ratios for $\alpha_{01,01}$ and $\alpha_{11,11}$ (1.033 and 1.037, respectively).¹⁰ From the estimated dynamic-to-static ratio of 1.035 for $\alpha_{01,11}$, one obtains the value $A = 0.21 \times 10^{-10}$ cm² for the dispersion parameter in Eq. (5). This allows us to mimic the experimentally measured polarizability ratio $|\alpha_{01,21}/\alpha_{01,11}|$ by using the value of $\alpha_{01,21}$ at $(\omega_p + \omega_s) = 2\omega$ as is, but adjusting $\alpha_{01,11}$ to the value it would have at $(\omega_p + \omega_s) = 2\omega + (\Omega_{01,21} - \Omega_{01,11})$, where ω is the frequency at which the *ab initio* calculation was actually done. This gives the ratio at fixed ω_p . The required dispersion adjustment to the *ab initio* value of $\alpha_{01,11}$ calculated at $\lambda = 488.0$ nm is $A [(\nu_p + \nu_s)^2 - (2\nu)^2] = 0.71\%$. The adjusted *ab initio* ratio $|\alpha_{01,21}/\alpha_{01,11}|$ is given in Table II and also plotted in Fig. 1. The calculated point lies just 1.8% above the experimental line. The small discrepancy between theory and experiment in this case is probably not significant.

The present experimental results and the various theoretical estimates of the ratios of overtone and fundamental transition polarizabilities for H₂ differ by 1.8, 11, and 18%. These discrepancies for H₂ are not nearly as large as the previously reported discrepancy for D₂.³ The single data point from the calculation of LeRoy and Schwartz¹⁰ is in good agreement with the experimental results for the first overtone. In the light of the present results it seems likely that the previously measured D₂ Raman intensities were incorrectly calibrated and should be remeasured. As a further test, it would be interesting to compare the results of the Le Roy and Schwartz calculation with experiment for the second overtone as well. Calculation of the relevant matrix elements at several frequencies would also allow one to compare *ab initio* and experimental dispersion curves for the polarizability ratios. It seems probable that the matrix elements for the rotational and the fundamental vibrational Raman transitions from low-lying levels of H₂ and all its isotopic forms, obtained in the calculations of Le Roy and Schwartz, are accurate to 0.1% or better; matrix elements at a range of frequencies for a few of the low-lying states of H₂ from such a calculation would be the definitive reference for the absolute calibration of gas phase Raman intensities.

Both the static⁹ and dynamic¹⁰ *ab initio* calculations use similar techniques and employ a large basis set of explicitly electron-correlated functions. The calculation of Le Roy and Schwartz uses a larger basis (249 terms¹⁰ vs 80 terms^{9,13}) to describe the clamped-nucleus electronic wave functions from which the effective internuclear potential is computed. Both calculations determine vibrational wave functions by numerical integration, taking care to ensure that the effective potential is smooth and accurate over a wide range of the internuclear distance R . Since the vibrational wave functions involved in overtone transitions are nearly orthogonal, the results are very sensitive to small inaccuracies of the potential. The function $\alpha(\omega; R)$ is obtained in each case from a

separate calculation; again, the $\alpha(\omega;R)$ assumed by Le Roy and Schwartz was calculated using a larger basis set of unperturbed and perturbed electronic functions (80 and 65 terms⁵ vs 54 and 34 terms¹⁴). It would be interesting to determine whether the higher accuracy of the overtone polarizabilities from the calculation of Le Roy and Schwartz may be attributed to the improved accuracy of the vibrational wave functions $|\nu J\rangle$ or to the improved polarizability function $\alpha(\omega;R)$. This has some bearing on the assessed accuracy of the calculated quadrupole moment matrix elements for H₂,¹³ since they are also very sensitive to the accuracy of the vibrational wave functions employed in their evaluation.

¹W. Holzer and R. Ouillon, *Chem. Phys. Lett.* **24**, 589 (1974).

²D. L. Rousseau, J. M. Friedman, and P. F. Williams, in *Topics in Current*

Physics, Raman Spectroscopy of Gases and Liquids, edited by A. Weber (Springer, Berlin, 1979), Vol. 11, p. 204.

³W. Knippers, K. van Helvoort, and S. Stolte, *Chem. Phys. Lett.* **121**, 279 (1985).

⁴D. M. Bishop and L. M. Cheung, *J. Chem. Phys.* **72**, 5125 (1980).

⁵J. Rychlewski, *J. Chem. Phys.* **78**, 7252 (1983).

⁶H. W. Schrotter and H. W. Klockner, in *Topics in Current Physics, Raman Spectroscopy of Gases and Liquids*, edited by A. Weber (Springer, Berlin, 1979), Vol. 11, p. 123.

⁷R. Ouillon and S. Adam, *J. Raman Spectrosc.* **12**, 281 (1982).

⁸*Handbook of Chemistry and Physics*, edited by R. C. Weast (Chemical Rubber, Boca Raton, 1987).

⁹J. L. Hunt, J. D. Poll, and L. Wolniewicz, *Can. J. Phys.* **62**, 1719 (1984).

¹⁰R. J. Le Roy and C. Schwartz, University of Waterloo Chemical Physics Research Report No. CP-301R (unpublished 1987); C. Schwartz and R. J. Le Roy, *J. Mol. Spectrosc.* **121**, 420 (1987).

¹¹D. A. Long, *Raman Spectroscopy* (McGraw-Hill, New York, 1977).

¹²R. Loudon, *The Quantum Theory of Light* (Clarendon, Oxford, 1983).

¹³J. D. Poll and L. Wolniewicz, *J. Chem. Phys.* **68**, 3053 (1978).

¹⁴W. Kolos and L. Wolniewicz, *J. Chem. Phys.* **46**, 1426 (1967).